Chapter 2
An Improved Fatigue Damage Spectrum for MIMO Random Testing

Enrico Proner and Emiliano Mucchi

Abstract This study focuses on Multiple-Input Multiple-Output (MIMO) vibration control tests, designed to accurately mimic a structure's operational vibration environment. In MIMO random testing, the Cross Spectral Density (CSD) between each pair of control channel plays a key role in the outcome of the test. In fact, the same Power Spectral Densities (PSDs) but with different CSDs may determine a different response on the Device Under Test (DUT) and different drives required to conduct the test. In this scenario, this paper proposes a methodology that aim to replicate a random vibration environment at the component level with minimal excitation. The approach pre-defines the phase and correlation of the reference Spectral Density Matrix (SDM) that maximize the response of the DUT. Then, the reference SDM is completed with the minimum PSD values ensuring that the structure's response in the laboratory aligns with the target vibration environment. This method enhances the consistency of laboratory tests with actual operational environments while minimizing the required energy, ultimately preserving the excitation system's integrity. The paper provides both a theoretical and an experimental analysis of the proposed methodology. The experiments are carried on specifically designed specimen excited by a multi-axis vibration environment, provided by a three-axis shaker.

Keywords Multi-axis test tailoring · Random testing · Fatigue · Fatigue Damage Spectrum · Environmental testing

Introduction

One way to assess the durability of a component is to conduct random vibration tests, which aim to mimic the operational environment by means of random excitation. In general, it is unfeasible to conduct life-long tests, therefore, the vibration environment is usually exaggerated in order to accelerate the test, overcoming time and costs limitations.

Typically, the test profiles are derived from Standards [1, 2]. However, standard profiles are generally much more severe than real vibration environments and may lead to over-testing. The best way to conduct the test is to adopt tailoring techniques [3]. These techniques require to gather operational data to synthesise vibration profiles that are more representative of the operational environment. Nowadays, the most accredited tailoring procedure is the one proposed by Lalanne [4] . Lalanne formalized two types of frequency spectra: the *Extreme Response Spectrum (ERS)* and the *Fatigue Damage Specteum (FDS) [5]*. According to Lalanne, the test article is represented by a of Single-Degree-of Freedom (SDOF) systems, with varying natural frequency in the bandwidth of interest. he vibration environment is applied as excitation to the base of the SDOF system. The FDS for a random excitation can be computed as:

$$FDS(fn) = \frac{n_0^+ T}{C} K^b \left(\sqrt{2} z_{rms}(f_n)\right)^b \Gamma\left(1 + \frac{b}{2}\right) \quad (1)$$

where n_0^+ is the mean number of zero up-crossing, z_{rms} is the root mean square of the SDOF relative displacement and Γ is the gamma function. In particular, the *FDS* represents the damage potential of a vibration environment. Procedures based on the equivalence of the *FDS* are widely studied and researched [6–11]. The formulation of the *FDS* is limited to uni-axial excitations, therefore, it neglects the possibility of multi-axis tests. However, real vibration environments are, in general, multi-axial. Moreover, in the recent past, multi-axis tests have been proven to be more realistic and more severe than traditional single-axis testing procedures [12, 13]. In this context, this paper investigates the possibility of a novel

Enrico Proner · Emiliano Mucchi
Department of Mechanical Engineering, University of Ferrara, Italy, Via Saragat 1
e-mail: enrico.proner@unife.it; emiliano.mucchi@unife.it

Alexandra Karlicek et al. (eds.), *Dynamic Environments Testing, Vol. 7*, Conference Proceedings of the Society for Experimental Mechanics Series, https://doi.org/10.13052/97887-438-0152-8_2

formulation of the *FDS*, suitable for multi-axis random excitations. In particular the *Multi-Input FDS (MI-FDS)* is presented. The *MI-FDS* takes into account the CSDs between multiple excitations, allowing to identify the real damage potential of a multi-axis random vibration. Moreover, this work provides the experimental verification of the *MI-FDS*. The experimental verification demonstrates the ability of the *MI-FDS* to evaluate the damage potential of multi-axis vibration environments, which enables the possibility of more accurate multi-axis tests.

The novel proposal: *Multi-Input Fatigue Damage Spectrum*

In this section the novel *MI-FDS* is presented. The general concept of the *MI-FDS*, compared to the traditional *FDS*, is described in Figure 1 .

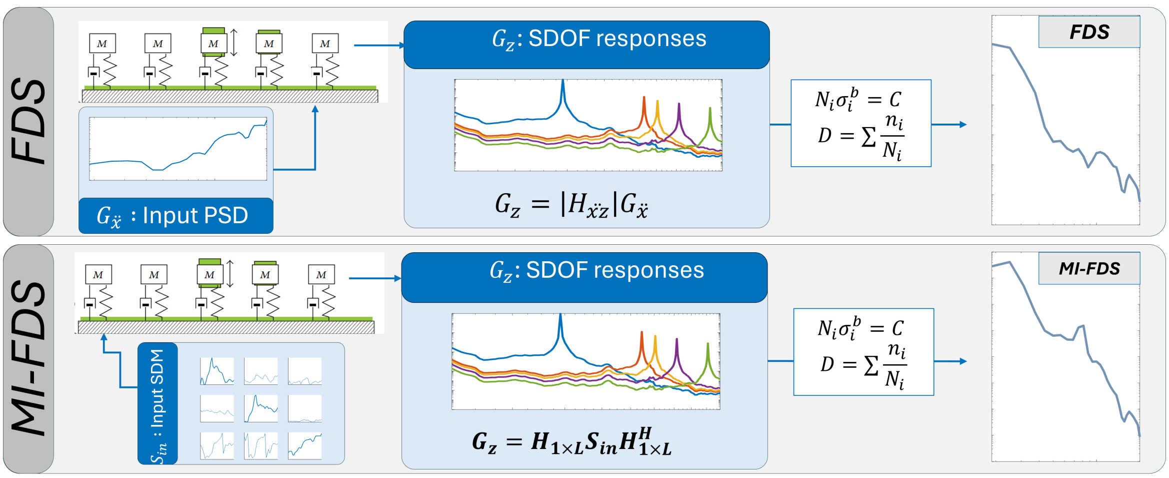

Fig. 1 Comparison between the calculation of the MI-FDS and *FDS* for a random vibration environment.

The *MI-FDS* shares most of the assumptions of the traditional *FDS*. However, the *MI-FDS* considers multiple simultaneous excitations applied to the SDOF system. As a consequence, the total response PSD of the SDOF system G_z subjected to multiple random excitations can be expressed as:

$$G_z = \mathbf{H_{1\times L} S_{in} H_{1\times L}^H} \tag{2}$$

where $\mathbf{H_{1\times L}}$ is the $1 \times L$ transfer function of the system , $\mathbf{S_{in}}$ is the $L \times L$ excitation Spectral Density Matrix (SDM) and the superscript ^{H} indicates the complex conjugate transpose operator. Each element of $\mathbf{H_{1\times L}}$ is computed as a frequency response function with amplitude:

$$|H_{\ddot{x}z}(f, f_n)| = \frac{1}{(2\pi f_n)^2 \sqrt{\left(1 - \left(\frac{f}{f_n}\right)^2\right)^2 + \left(2\zeta \frac{f}{f_n}\right)^2}} \tag{3}$$

and phase:

$$\angle H_{\ddot{x}z}(f, f_n) = atan\left(\frac{2\zeta f f_n}{f_n^2 - f^2}\right) \tag{4}$$

Equation (2) can be also expressed in terms of phases and coherences of $\mathbf{S_{in}}$:

$$G_z = \Sigma_{j=1}^{L} S_{in,jj} W_{jj} + 2\Sigma_{j=1}^{L-1}\Sigma_{k=j+1}^{L}\sqrt{\gamma_{jk}^2 S_{in,jj} S_{in,kk}}|W_{jk}|cos\left(\phi_{jk} - \xi_{jk}\right) \tag{5}$$

where $\mathbf{W} = \mathbf{H_{1\times L}^H H_{1\times L}}$, ξ_{jk} is the phase of Wjk, γ_{jk} is the coherence and ϕ_{jk} is the phase of $S_{in,jk}$. In Equation (5) the phase and coherence of the excitation SDM are explicit. In particular, γ_{jk} and $cos\left(\phi_{jk} - \xi_{jk}\right)$ defines how much the j^{th} and k^t excitation are combined constructively or destructively to increase or decrease the response of the SDOF system.

Moreover, it should be noted that the phase difference between $S_{in,jk}$ and W_{jk} is specific of the SDOF system. Therefore, the value $\phi_{jk} - \xi_{jk}$ must be coherent between the test and the SDOF system to guarantee the consistency of the calculated damage potential. The resulting response of Equation (5) can be used to compute the *MI-FDS*:

$$\textit{MI-FDS} = \frac{n_0^+ T \sqrt{2^b}}{C} K^b \left(\int_0^\infty G_z df \right)^b \Gamma \left(1 + \frac{b}{2} \right) \tag{6}$$

Experimental Verification

In this section the experimental verification of the *MI-FDS* is presented. The objective of the test campaign is to demonstrate the capability of the *MI-FDS* to take into account the phase and coherence between multiple simultaneous random excitation and provide an accurate evaluation of the damage potential of multi-axis vibration environments. The first part of this section is dedicated to the presentation of the experimental set up and the results of the testing campaign. In the second part, the results of the experimental campaign will be discussed.

Test set up and results

The specimen chosen for the test campaign is a cantilever aluminum beam with rectangular section and U-shaped notches near the fixed end. A lumped mass of 0.47 kg is placed on the free-end of the beam, to tune its natural frequencies in a convenient frequency range. The detailed geometry of the beam is depicted in Figure 2. The excitation system used for the test campaign is the three-axial electro-dynamic shaker available at University of Ferrara. This excitation system is composed of three actuators (10 kN each) that allow to excite the specimen mounted on the head expander along three orthogonal translational DOFs. Figure 3. SCADAS Mobile SCM202V and MIMO Random of Simcenter Testlab are used as data acquisition hardware and vibration control software, respectively. The control accelerometer (model 356B21 by *PCB Piezotronics*) is placed on the fixture, near the fixed end of the cantilever beam. In addition, an accelerometer is placed on the tip of the beam to monitor the response of the specimen.

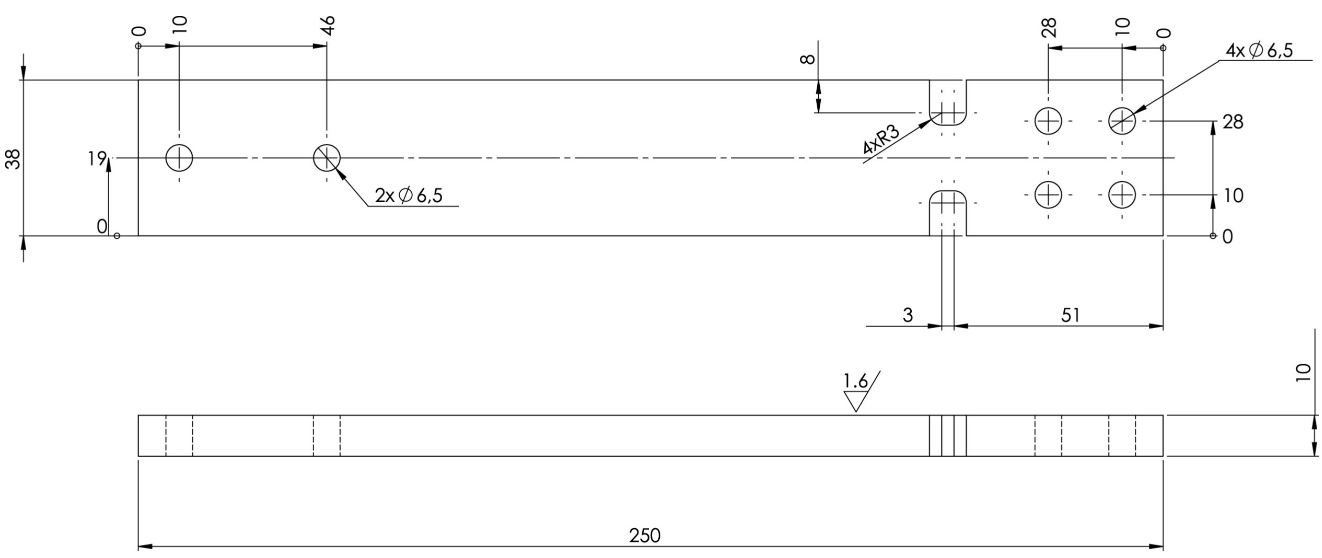

Fig. 2 Detailed geometry of the specimen used in the testing campaign (all measures are in *mm*).

The objective of the experimental campaign is to obtain the Time-to-Failure (TTF) of the specimen under different types of vibration environments. In particular, a reference vibration environment is defined in the $[25 - 200]Hz$ bandwidth. Then, the traditional *FDS* and the novel *MI-FDS* are used to generate equivalent tests. Four kinds of test are carried out, each one repeated on three specimens and conducted until total failure:

1. Test Environment 0 (TE-0): three-axial reference vibration environment.
2. Test Environment 1 (TE-1): synthesise three separate PSDs to have the same *FDS*, computed according to Equation (1), and the same TTF of TE-0. The obtained PSDs are applied separately and sequentially to the specimen for a duration

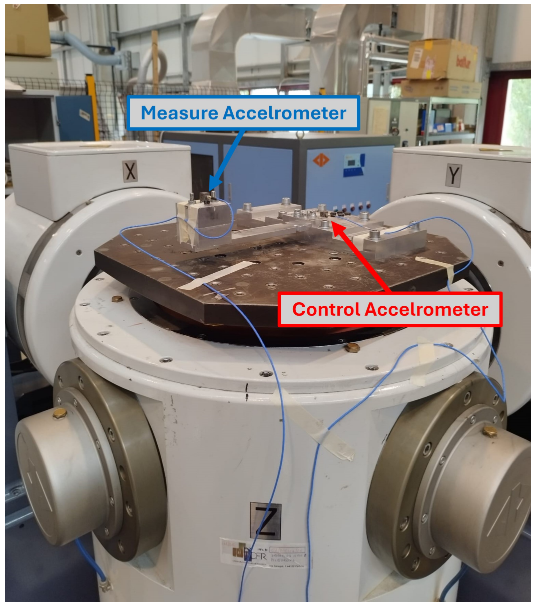

Fig. 3 Specimen mounted on the shaker.

equal to the mean TTF of TE-0. If the specimen survives the first sequence of excitations, the test is performed again until failure.

3. Test Environment 2 (TE-2): the PSDs obtained for TE-1 are applied simultaneously to the specimen. The phase and coherence between each axis is defined according to the *Extreme Dynamic Response Method (EDRM)* [14].
4. Test Environment 3 (TE-3): The vibration environment of TE-2 is scaled to have the same *MI-FDS*, computed according to (6), and the same TTF of TE-0.

The SDM of TE-3 is obtained according to the following equation:

$$\mathbf{S_{in_{TE-3}}} = \frac{\textit{MI-FDS}_{TE-0}}{\textit{MI-FDS}_{TE-2}} \mathbf{S_{in_{TE-2}}} \tag{7}$$

where $\mathbf{S_{in_{TE-3}}}$ and $\mathbf{S_{in_{TE-2}}}$ are the excitation SDM of TE-3 and TE-2 and $\textit{MI-FDS}_{TE-0}$ and $\textit{MI-FDS}_{TE-2}$ are the *MI-FDS* of TE-0 and TE-2. The resulting vibration environment is a SDM with the same phase and coherence of TE-2 but with the PSDs that match the *MI-FDS* of TE-0. Figure 4 shows the SDM of TE-0 (solid blue), TE-2 (dashed red) and TE-3 (dashed green). The plots on the diagonal show the excitation PSD along each-axis. The upper triangular plots show the coherence, the lower triangular plots the phase between each pair of excitations.

Figure 5 shows the *FDS* (left plot) and *MI-FDS* (right plot) computed for each test environment. The parameters used for the computation of the *FDS* and the *MI-FDS* are $b = 5.4$, $C = 5.1 \cdot 10^{17}$ and a damping ratio of $\zeta = 0.1\%$. In the plot on the left, the total *FDS* of each test environment is depicted. TE-0, TE-1 and TE-2 are represented by the same curve (dashed gray). The blue curve depicts the *FDS* computed for TE-3. The total *FDSs* are obtained by summing the *FDSs* of each single-axis excitation. The plot on the right shows the *MI-FDS* computed for TE-0 (blue curve), TE-1 (gray curve), TE-2 (red curve) and TE-3 (green curve), computed according to Equation (6).

Finally, Table 1 shows the TTFs obtained for each specimen in the testing campaign. The TTFs from Table 1 are also depicted in the box plot of Figure 6. In Figure 6, each box describes the first quartile of the TTFs obtained from each test environment, the red line and the black cross are the median and the mean of the TTFs, respectively.

Discussion of the results

The first result that needs to be addressed is the difference between the traditional *FDS* and the novel *MI-FDS*. In Figure 5, in the left plot, the total *FDS* computed for TE-0, TE-1 and TE-2 is the same. In fact, the traditional *FDS* considers only the PSD of each excitation. TE-0, TE-1 and TE-2 excite the system with the same PSDs, therefore, the total *FDS* is the same for these test environments. Moreover, the total *FDS* of TE-3 resulted lower than the the total *FDS* of TE-0, as the PSDs of TE-3 are lower. On the other hand, the *MI-FDS* produces three distinct curves for TE-0, TE-1 and TE-2. In particular TE-1

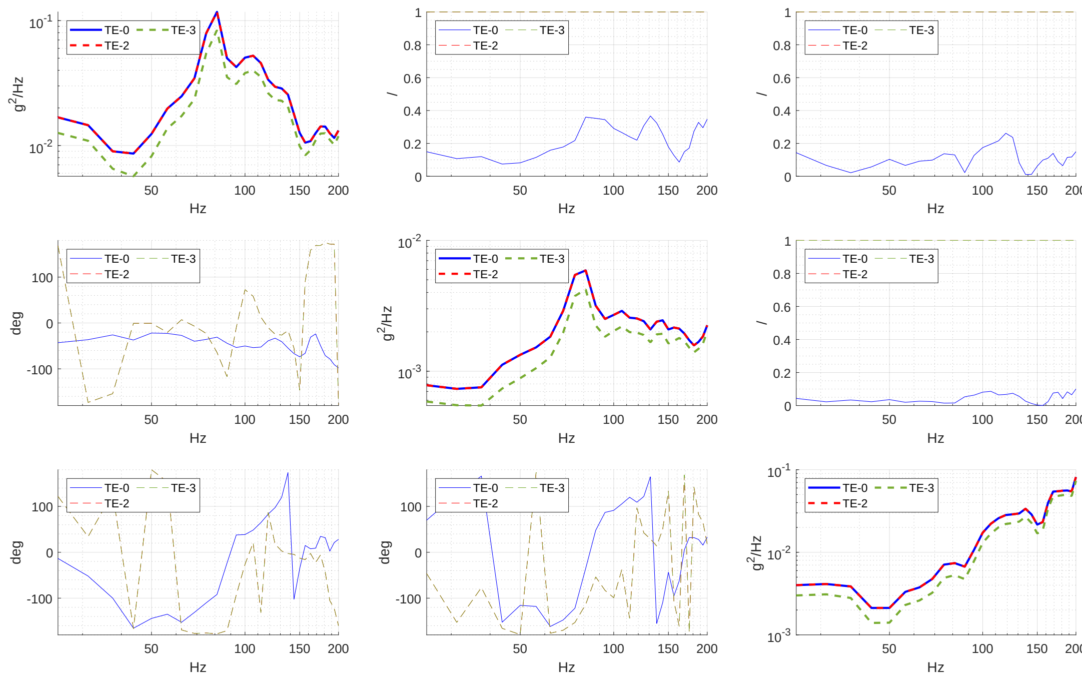

Fig. 4 SDM of the TE-0 (solid blue) ,TE-2 (dashed red) and TE-3 (dashed green)

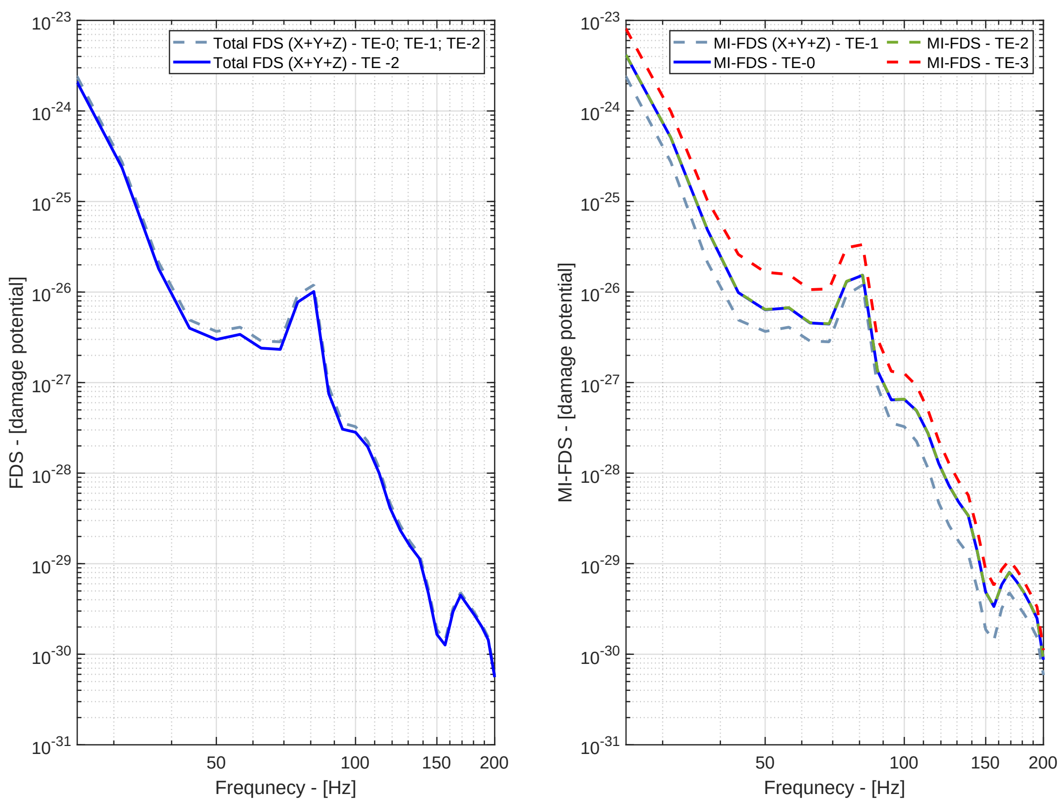

Fig. 5 FDS (left) and MI-FDS (right) of the tests

Table 1 TTFs obtained in the testing campaign

	Time-to-Failure - [s]				
	spec #1	**spec #2**	**spec #3**	**Mean**	**Standard dev.**
TE-0	1537	1620	1920	1692,3	201,4
TE-1	6036	5265	5522	5607,6	392,5
TE-2	1380	1292	1008	1226,6	194,4
TE-3	1648	1818	1472	1646,0	173,0

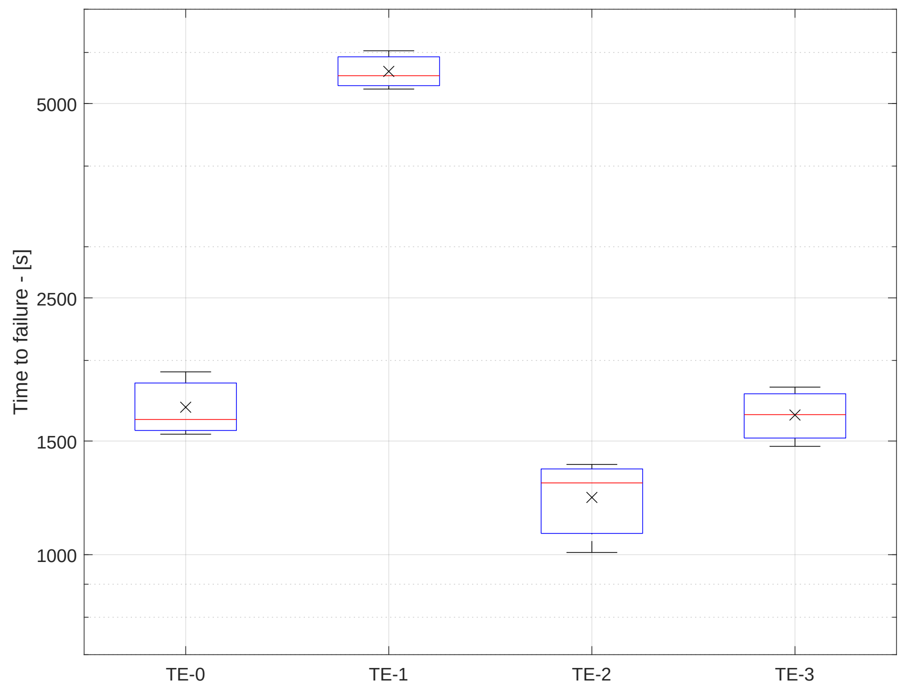

Fig. 6 Box plot of the TTFs obtained in the test campaign

has the lowest damage potential. This is expected, as the combination of multiple simultaneous excitations determines a greater response of the tested system, resulting in a higher damage output [15–17]. The highest damage potential, according to the *MI-FDS*, is given by TE-2. In Equation (6), $cos\left(\phi_{jk} - \xi_{jk}\right)$ and γ_{jk} are both equal to 1 for TE-2. In fact, the phases and coherences of the SDM of TE-2 are set according to the EDRM, which maximize the response of the system and, therefore, achieves the maximum damage potential. Moreover, the *MI-FDS* of TE-0 is lower than the one of TE-2 as the correlation between the excitations determines a lower response of the system. Finally, TE-3 has been obtained to match the *MI-FDS* of TE-0, with the phases and coherences of TE-2. The PSDs of TE-3 are lower than the ones of TE-0, however, the contribution of the CSDs determines an increased response of the system that allows to match the *MI-FDS* of TE-0. The previous consideration imply the following predictions regarding the outcome of the tests:

1. According to the traditional *FDS*: TE-0, TE-1 and TE-2 will be equally damaging to the specimen while TE-3 will be the least damaging environment.
2. According to the novel *MI-FDS*: TE-1 will be the least damaging test, TE-2 will be the most damaging test, TE-0 and TE-3 will deliver the same damage to the specimen.

These predictions are now compared to the actual outcome of the tests, described by Table 1 and Figure 6. The results of the testing campaign demonstrate that the predictions made according to the *MI-FDS* are correct. In fact, in comparison to the mean TTF of TE-0, TE-1 determined a 231$\%$ increase in the TTF, TE-2 caused a 27$\%$ reduction of the mean TTF and, finally, the mean TTF of TE-3 deviates form the mean TTF of TE-0 by only 2.7$\%$. These results are depicted in Figure 6. It can be seen that TE-1 determined the highest TTFs (least damage), while TE-2 determined the lowest TTFs (most damage), in accordance to the prediction made by the *MI-FDS*. Moreover, TE-0 and TE-3 determined very similar TTFs distributions. This result indicates that, although the PSDs of the TE-3 are lower than the PSDs of TE-0, the damage output of TE-3 is the same of TE-0. This is to be attributed to the contribution of the CSDs, which allow TE-3 to have the same *MI-FDS* of TE-0 but with lower PSDs.

The analysis of the obtained TTFs confirms that the predictions made according to the *MI-FDS* reflect the experimental results of the testing campaign. Therefore, the *MI-FDS* correctly takes into account the contribution of the CSDs of multi-axis random vibration environments to the fatigue damage inflicted to the specimen. Furthermore, the *MI-FDS* has been able to modify TE-2 to generate a new vibration environment that deals the same damage as TE-0 to the specimen in the same amount of time. Finally, the test campaign demonstrates the incapability of the traditional *FDS* approach to evaluate multi-axis vibration environments. In fact, the *FDS* could not distinguish TE-0, TE-1 and TE-2, which have the same PSDs but dealt different damage to the specimen.

Conclusion

In this paper a new approach to the Fatigue Damage Spectrum has been investigated. The *Multi-Input FDS* is proposed, to consider the correlation of multiple simultaneous random excitations in the computation of the damage potential of a multi-axis vibration environment. The validity of the proposed approach has been tested in a dedicated test campaign. In particular, ad-hoc designed specimens have been tested until failure under different vibration environments and the *MI-FDS* has been used to evaluate the damage potential of each vibration environment. The proposed approach allowed to make predictions on the outcome of the tests coherent with the experimental results. In fact, the *MI-FDS* was able to correctly identify the most and least damaging environments and recognised the environments that determine the same damage output. Moreover, the *MI-FDS* allowed to synthesise a new vibration environment equally damaging to the tested article as the reference vibration environment. The experimental results proved that the *MI-FDS* offers a significant improvement over the traditional *FDS* in evaluating the damage potential of multi-axis random vibrations.

References

1. NSA. “Environmental conditions”. *AECTP 200, category 240* (2006)
2. de la Defense Delegation Generale pour l’armement, M. “Essais generaux en environment des materials (general tests of materials in environment)”. *GAM EG-13*.
3. of Defence, U.S.D. “Environmental engineering considerations and laboratory tests. method 527.1: Multi-exciter test”. *MIL-STD 810G w/CHANGE 1*.
4. Lalanne, C. “Specification development, third ed.”. *John Wiley & Sons, Inc - ISTE, London* (2014)
5. Lalanne, C. “Maximum response and fatigue damage spectra – part i & part ii”. *The journal of environmental sciences, July/Augst* (1984)
6. Xu, F., Ahlin, K., and Wang, B. “Optimization of damage equivalent accelerated test spectrum derivation using multiple non-gaussian vibration data”. *Journal of Sensors*, 2021(1):3668726 (2021)
7. Coutinho, I.A. and Landre Jr, J. “Enhanced tailored durability test specification for multiaxial dynamically excited structures attached to a single input base under off-road loading environment”. *Engineering Structures*, 219:110768 (2020)
8. Decker, M., Kinscherf, S., Bauer, N., David, P., and Serifsoy, M. “Deriving fatigue equivalent power spectral density spectra for the vibration testing of engine components”. *Materialwissenschaft und Werkstofftechnik*, 49(3):392–405 (2018)
9. Cianetti, F., Alvino, A., Bolognini, A., Palmieri, M., and Braccesi, C. “The design of durability tests by fatigue damage spectrum approach”. *Fatigue & Fracture of Engineering Materials & Structures*, 41(4):787–796 (2018)
10. Angeli, A., Cornelis, B., and Troncossi, M. “Synthesis of sine-on-random vibration profiles for accelerated life tests based on fatigue damage spectrum equivalence”. *Mechanical Systems and Signal Processing*, 103:340–351 (2018)
11. Aimé, M., Banvillet, A., Khalij, L., Pagnacco, E., Chatelet, E., and Dufour, R. “A framework proposal for new multiaxial fatigue damage and extreme response spectra in random vibrations frequency analysis”. 213 (2024)
12. Proner, E., Mucchi, E., and Tovo, R. “A relationship between fatigue damage estimation under multi-axis and single-axis random vibration”. *Mechanical Systems and Signal Processing*, 215:111402 (2024)
13. Nath, N. and Aglietti, G.S. “Study the effect of tri-axis vibration testing over single-axis vibration testing on a satellite”. In *2022 IEEE Aerospace Conference (AERO)*, pages 1–10 (2022)
14. D’Elia, G., Mucchi, E., and Dalpiaz, G. “A novel methodology for dynamic response maximisation in multi-axis accelerated random fatigue testing”. 181 (2022)
15. Gregory, D., Bitsie, F., and Smallwood, D. “Comparison of the response of a simple structure to single axis and multiple axis random vibration inputs” (2008)
16. Whiteman, W. and Berman, M. “Inadequacies in uniaxial stress screen vibration testing”. *Journal of the IEST*, 44:20–23 (2001)
17. French, R., Handy, R., and Cooper, H. “A comparison of simultaneous and sequential single-axis durability testing” (2006)